Eur Biophys J (2001) 30: 186–197
DOI 10.1007/s002490100138

ARTICLE

Normann Spitzner · Frank Löhr · Stefania Pfeiffer
Assen Koumanov · Andrey Karshikoff · Heinz Rüterjans

Ionization properties of titratable groups in ribonuclease T_1

I. pK_a values in the native state determined by two-dimensional heteronuclear NMR spectroscopy

Received: 22 August 2000 / Revised version: 21 December 2000 / Accepted: 21 December 2000 / Published online: 13 March 2001

Abstract pK_a values of amino acid side chains of ribonuclease T_1 have been determined from the pH dependence of ^{13}C and ^{15}N resonances. It was possible to derive pK_a values of single protonation or deprotonation sites of carboxylate and imidazole groups. Deviations from pK_a values of free amino acids could be interpreted with electrostatic interactions of corresponding side chains with the protein environment. In particular, the interaction between H27 and E82 led to an increase of the H27 pK_a and a decrease of the E82 pK_a. The pK_a of E28 at the C-terminal end of the α-helix was increased because of the dipolar character of the α-helix. D76 did not titrate in the investigated pH range of about 2–9. From the chemical shift value this buried side chain seems to be protonated. The pK_a values of side chains in the active site deviate from a normal behaviour. The lower pK_a value of E58 may be interpreted with the close proximity of this side chain with positively charged H40 and R77. A novel two-dimensional $^1H(^{13}C^{\delta})^{13}C^{\gamma}$ correlation experiment was developed to observe the pH dependence of the chemical shifts of the C^{γ} resonances of histidine residues. From the inspection of the C^{γ} chemical shift-pH profiles it was possible to determine the predominant tautomeric form for the histidine residues at higher pH values.

Keywords Ribonuclease T_1 · pH titration · pK_a values · Histidine tautomer formation · Nuclear magnetic resonance

N. Spitzner · F. Löhr · S. Pfeiffer · H. Rüterjans (✉)
Institut für Biophysikalische Chemie,
Johann Wolfgang Goethe-Universität, Biozentrum N230, 1 OG,
Marie-Curie-Strasse 9, 60439 Frankfurt a.M., Germany
E-mail: hruet@bpc.uni-frankfurt.de
Tel.: +49-69-79829630
Fax: +49-69-79829632

A. Koumanov · A. Karshikoff
Karolinska Institute, Department of Biosciences at Novum,
141 57 Huddinge, Sweden

Introduction

Electrostatic interactions in proteins are usually of utmost importance for their functional properties, be it enzyme activity or protein-ligand interactions. Since the number of charges in proteins depends on pH, the ionization behaviour of titratable groups can be derived from experimental pK_a values of amino acid side chains. In very early investigations, group pK_a values were obtained from potentiometric titrations of proteins (Linderstrøm-Lang 1924). In later years, pH-dependent spectroscopic changes were used for the determination of individual pK_a values (Edsall et al. 1958). In particular, ^1H NMR resonances have been followed with pH for pK_a values of histidine side chains (Bradbury and Scheraga 1966; Meadows et al. 1968; Rüterjans and Witzel 1969). In addition, the tautomeric state of the deprotonated imidazole ring system of histidines could be determined from corresponding pH-dependent ^{13}C and ^{15}N resonances (Reynolds et al. 1973; Blomberg et al. 1977). Recently, two- and three-dimensional heteronuclear NMR experiments have been applied to the determination of carboxylate pK_a values of aspartate and glutamate residues in proteins (Oda et al. 1994; Yamazaki et al. 1994).

Previous attempts have been made to calculate pK_a values of proteins. Of particular interest were deviations of pK_a values of titratable groups from those observed for free amino acids or model compounds. Taking into account interactions between side chains via hydrogen bonds rather than by electrostatic interactions, Laskowski and Scheraga (1954) tried to correlate observable pK_a values with microscopic association constants between side chains of opposite charges. In recent years the electrostatic properties of proteins have been the subject of many theoretical treatments (for reviews see Gilson 1995; Nakamura 1996; Warshel and Papazyan 1998; Ullmann and Knapp 1999). The problem is that the equilibrium between the ionized and the neutral states in aqueous solution is determined by a

large number of interactions with the solvent water, with neighbouring charges or permanent dipoles of the protein. The theoretical analysis of these factors is hampered by the lack of experimental data for determining pK_a values in proteins. The lack of data is certainly also connected with the destabilization of protein structures upon a titration of amino acid side chains. Most of the proteins unfold when the pH value decreases beyond the pK_a values of the carboxylate groups. Alternatively, proteins tend to denature when tyrosine or lysine side chains are titrated at high pH values.

Since ribonuclease T_1 (RNase T_1) belongs to the very few proteins which are stable in the pH range 2–9, this enzyme was chosen as an appropriate model protein for the determination of pK_a values of carboxylate and imidazole side chains. The crystal structure and the solution structure have been determined with a high degree of accuracy (Martinez-Oyanedel et al. 1991; Pfeiffer et al. 1997). In previous studies, pK_a values of the three histidines have been determined from the pH dependence of the $^1H^{\varepsilon 2}$ proton resonances of the imidazole ring systems (Rüterjans et al. 1969; Rüterjans and Pongs 1971; Fülling and Rüterjans 1978). From deviations in the titration curves and from abnormal pK_a values it has been suggested that at least two of the histidines interact with neighbouring carboxylate side chains at neutral pH values. In later work, ^{15}N labelling was intended to allow for a more sensitive determination of pK_a values (Schmidt 1990). Unfortunately, the titration behaviour and the tautomeric states could not be determined utilizing the pH dependence of ^{15}N imidazole resonances owing to extensive line broadening above pH 7. This line broadening is probably the result of interconversion of the two tautomeric forms at intermediate rates on the NMR time scale. Indeed, the expected changes of the ^{15}N imidazole chemical shifts of about 80 ppm (Blomberg et al. 1977) are certainly responsible for this effect.

So far, no pK_a values of aspartate and glutamate residues of RNase T_1 were determined by NMR spectroscopy. Therefore this model enzyme (for reviews see Pace et al. 1991; Steyaert 1997) was chosen to probe the titration behaviour of side chain carboxylates from pH 2 to pH 9 using two-dimensional ^1H-^{13}C correlation NMR spectroscopy, and thereby to reinvestigate the pK_a values of histidine residues. Furthermore, this study was intended to assess the tautomeric state of the deprotonated imidazole ring system of the three histidines. For this purpose it was necessary to develop a NMR experiment allowing a quick and more convenient detection of the histidine C^γ resonances. In this first paper, the experimental protonation/deprotonation equilibria of the carboxylate groups and the histidines in RNase T_1 are presented. In the second following paper, an analysis of the pK_a values of these groups calculated on the basis of a continuum dielectric model will be described and the agreement with experimental results is discussed.

Materials and methods

Protein preparation

Uniformly $^{13}C/^{15}N$ labelled Lys25-ribonuclease T_1 was expressed in *Escherichia coli* strain DH5α transformed with the plasmid pA2T1 harbouring a chemically synthesized gene for RNase T_1 (Quaas et al. 1988a, 1988b). $^{13}C/^{15}N$ enrichment was achieved by growing the bacteria in a modified M9 medium with $^{15}NH_4Cl$ (1 g/L) and [$^{13}C_6$]-D-glucose (2 g/L) as the sole nitrogen and carbon sources, respectively. Fed-batch cultivation of DH5α/pA2T1 with a controlled glucose feed led to a yield of 14 mg/L of purified enzyme. The recombinant protein was prepared as described previously (Schmidt et al. 1991) with the following modifications. In the first step, RNase T_1 was released from the periplasm by sonication and in the last step it was desalted by gel filtration (Sephadex G15, 3×140 cm), and then lyophilized. The purity of the enzyme was checked by UV spectroscopy and analytical HPLC, both on a Mono Q HR 5/5 and a Superdex 75 HR 10/30 column. Protein samples for the NMR titration experiments were made 1.5 mM in a 500 μL final volume containing 90% H_2O and 10% D_2O.

NMR experiments

All 2D NMR spectra were recorded at 308 K on a Bruker Avance DMX 500 spectrometer equipped with an actively shielded *z*-gradient 5 mm triple-resonance $^{15}N/^{13}C/^1H$ probe head. In all experiments the ^1H carrier was placed on the water resonance frequency and ^{13}C decoupling during data acquisition was accomplished by GARP-1 modulation (Shaka et al. 1985). All spectra were acquired with 512 complex data points in the acquisition domain with a spectral width of 5000 Hz. Unless otherwise noted, States-TPPI phase cycling (Marion et al. 1989) was used for obtaining quadrature phase detection in the indirectly observed dimension and solvent suppression was achieved by including the WATERGATE module (Piotto et al. 1992) in the original pulse sequences.

The behaviour of the carboxyl and carboxamide side chain carbons of Asx and Glx as a function of pH was monitored using a two-dimensional version of the CT-HCACO experiment (Powers et al. 1991; Grzesik and Bax 1993), modified to optimize the observation of the $^1H^\beta(^{13}C^\beta)^{13}C^\gamma$ and $^1H^\gamma(^{13}C^\gamma)^{13}C^\delta$ correlations of all Asx and Glx residues, respectively (Yamazaki et al. 1994). The experiment was implemented with pulsed-field gradients for suppression of artifacts (Bax and Pochapsky 1992). Shaped pulses were used to excite aliphatic carbons with chemical shifts smaller than 50 ppm or carbonyl carbons selectively. The ^{13}C carrier frequency was set to 179 ppm. A total of 200 complex t_1 experiments was recorded with 64 scans per increment and a spectral width of 1852 Hz in the carbon dimension. The total measuring time was about 2.5 h. Zero-filling twice in t_2 and three times in t_1 yielded a digital resolution of approximately 2.4 Hz/point and 1.8 Hz/point in the ^1H and ^{13}C dimensions.

The pH titration behaviour of histidine ring carbons attached to a hydrogen atom was followed by means of a CT-HSQC experiment (Vuister and Bax 1992). This experiment was recorded in the sensitivity-enhanced version (Palmer et al. 1991), employing a heteronuclear gradient echo for coherence selection and water suppression (Kay et al. 1992). The ^{13}C carrier was positioned at 130 ppm and the spectral width covered 5000 Hz in the indirect dimension. Altogether, 64 complex t_1 experiments were acquired with 16 transients per each free induction decay, leading to a total acquisition time of approximately 40 min. Spectra with pure phases and frequency discrimination in the carbon dimension were obtained from the original data sets according to the way described by Kay et al. (1992). Zero filling was employed to reach final two-dimensional matrices of 1024×256 real data points, resulting in a digital resolution of approximately 4.9 Hz/point and 19.5 Hz/point in the ^1H and ^{13}C dimensions, respectively.

A novel two-dimensional $^1H^\delta(^{13}C^\delta)^{13}C^\gamma$ correlation experiment was used to investigate the pH dependence of the chemical shifts of

the C^{γ} resonances of histidine residues. The pulse scheme of this experiment, abbreviated as CT-H(CD)CG^{His}, utilized the same magnetization transfer pathway as the previously reported ^{13}C-^{13}C-^{1}H heteroSQC/homoSQC experiment (Yamazaki et al. 1993). However, a constant-time evolution period is employed in the CT-H(CD)CG^{His} in order to remove the splitting of the $^{13}C^{\gamma}$-$^{13}C^{\delta}$ spin coupling and, more importantly, to achieve a further attenuation of the phenylalanine and tyrosine aromatic signals relative to the histidine imidazole signals, exploiting the substantially larger histidine $^{13}C^{\gamma}$-$^{13}C^{\delta}$ coupling constant (ca. 70 Hz) in comparison with the aromatic $^{1}J_{CC}$ couplings (ca. 55 Hz) (Tran-Dinh et al. 1975). Details and further improvements of the pulse sequence, allowing the application to larger proteins, will be reported elsewhere (to be published). All spectra were acquired with 154 complex t_1 experiments, and 64 scans per increment. Total measuring times were about 3 h per spectrum. Spectral width comprised 5556 Hz in the carbon dimension and the ^{13}C carrier was set to 130 ppm. Zero filling once in t_2 and three times in t_1 led to a digital resolution of approximately 4.9 Hz/point and 5.5 Hz/point in the ^{1}H and ^{13}C dimensions.

A two-dimensional version of the CT-HCN experiment (Sudmeier et al. 1996), with pulsed-field gradients for artifact suppression, was utilized for the observation of the pH dependence of the chemical shifts of the imidazole nitrogens in the histidine residues. Parameters for this experiment included a ^{15}N sweep width of 7143 Hz centered at 189.8 ppm, 44 complex t_1 experiments and 320 scans per free induction decay. The total measuring time was about 6 h. The time domain data were zero filled to 256 real data points in the indirect dimension and 1024 real data points in the direct dimension prior to Fourier transformation. The resulting digital resolution was approximately 4.9 Hz/point in the ^{1}H dimension and 27.9 Hz/point in the ^{15}N dimension. A reduced ^{15}N sweep width of 3571 Hz was used for spectra recorded below pH 5, yielding a digital resolution of approximately 14 Hz/point.

All spectra were processed and analysed on an Aspect 3000 workstation using the programs UXNMR and AURELIA (Bruker Analytische Messtechnik, Karlsruhe). In general, shifted, squared sine-bell apodization functions were applied prior to Fourier transformation.

pH titration experiments

The effect of pH on selected ^{1}H, ^{13}C and ^{15}N chemical shifts in RNase T_1 was followed by analysing a series of the above-mentioned set of four NMR experiments recorded at 18 different pH values, ranging from pH 2.1 to pH 9.6. The pH was measured at 308 K by a PHM 210 Radiometer pH meter equipped with a Mettler Toledo InLab 423 micro combination pH electrode, and calibrated prior to use with standard buffer solutions of pH 4.01, 7.00 and 10.01 (Radiometer Copenhagen). The uncertainty in the pH measurements was assumed to be 0.05 pH units.

For the first NMR measurement, the sample was brought to pH 9.6 with the addition of 1 M NaOH. Subsequent pH adjustments were made with small volumes of 1 M HCl. For each pH adjustment, the NMR sample was transferred to a micro reaction vessel, the pH was varied by addition of aliquots of acid, and then used to be mixed with solution traces within the NMR tube. The equilibriated solution was returned to the micro reaction vessel, temperature-equilibriated for 10 min, and then the pH was measured. Values were redetermined directly after each set of NMR experiments, and never varied by more than 0.1 pH units. Averages of the initial and the final pH were recorded. Reported values were not corrected for the deuterium isotope effect. Owing to the experimental conditions the ionic strength never exceeded 40 mM. To test the reversibility of the titration the pH of the acidified sample was adjusted back to 9.6 and the set of NMR experiments was repeated.

pH-dependent chemical shift data analysis

^{1}H chemical shifts were referenced to the pH-independent γ-methylene proton resonances of Q85 at 2.10 ppm and 2.26 ppm as well as to the $^{1}H^{\alpha}$ resonance of N81 at 6.13 ppm (Pfeiffer et al. 1996), using the corresponding cross peaks in the 2D CT-H(CA)CO spectrum of RNase T_1 at pH 5.5. The ^{1}H chemical shifts are given relative to the 2,2-dimethyl-2-silapentane-5-sulfonate (DSS) standard and the ^{13}C and ^{15}N reference frequencies were calculated from the ^{1}H spectrometer frequency (Wishart et al. 1995). The estimated uncertainties of the chemical shifts used in the data analysis are 0.02 ppm and 0.1 ppm for ^{1}H and heteronuclei, respectively. Cross peaks were assigned in the spectra at pH 5.5 by reference to the reported chemical shift assignments at that pH (Pfeiffer et al. 1996). pH-dependent chemical shifts were then followed incrementally to pH 2.1 and pH 9.6, respectively.

The pH dependence of the chemical shift observed for an appropriate reporter nucleus near to or at a titratable site was fitted by modified Henderson-Hasselbalch equations describing up to four protonation/deprotonation processes, which were assumed to be independent (Shrager et al. 1972; Blomberg et al. 1977):

$$\delta(\mathrm{pH}) = \delta_b + \sum_{i=1}^{j} \left[C_i(\delta_a - \delta_b) 10^{(\mathrm{p}K_{a_i} - \mathrm{pH})} \right] \Big/ \left[1 + 10^{(\mathrm{p}K_{a_i} - \mathrm{pH})} \right]$$

$$\text{with } \sum_{i=1}^{j} C_i = 1 \text{ and } j = 1,\ 2,\ 3 \text{ or } 4 \qquad (1)$$

Here δ(pH) is the observed chemical shift for the resonance of the reporter nucleus at a given pH, while δ_a and δ_b denote the limiting chemical shifts of this resonance at acidic and basic pH. pK_{ai} is the negative common logarithm of the apparent acid dissociation constant for the ith protonation/deprotonation process reflected by the reporter resonance and the product $C_i(\delta_a–\delta_b)$ represents the contribution of this protonation/deprotonation step to the total chemical shift change ($\delta_a–\delta_b$). Also, the modified Hill equation for a one-step titration was used to simulate the experimental data (Markley 1975):

$$\delta(\mathrm{pH}) = \left[\delta_b + \delta_a \times 10^{n(\mathrm{p}K_a - \mathrm{pH})} \right] \Big/ \left[1 + 10^{n(\mathrm{p}K_a - \mathrm{pH})} \right] \qquad (2)$$

where n is the Hill coefficient, a probe of cooperativity between the ionization sites. p$K_{a(i)}$ values and additional parameters (C_i or n, δ_a, δ_b) were determined from the experimental data by the Levenberg-Marquardt nonlinear least-squares fitting procedure using the program MicroCal Origin, version 2.9 (MicroCal, Northampton, Mass., USA). The reported standard errors in the fitted parameters were calculated by the same software package. Therefore, these errors relate to the precision of the data fitting, but not to the accuracy of the fitting parameters.

The choice of the number i of protonation/deprotonation processes required to fit the experimental data to Eq. (1) was made mainly by F-test statistics (Motulsky and Ransnas 1987) using a confidence level of 99%. F-Tests were performed utilizing a MATLAB routine kindly provided by Dr. D. Fushman (College Park, Md., USA). Also, structural considerations were taken into account in a reliable determination of the number i of protonation/deprotonation processes. For this, distance measurements from reporter atoms to ionizing atoms were carried out for both the crystal structure (PDB code 9RNT) (Martinez-Oyanedel et al. 1991) and the solution structure ensemble (PDB code 1YGW) (Pfeiffer et al. 1997) of free ribonuclease T_1. Distance calculations and all molecular graphics were performed in MOLMOL, Windows NT version 2.5.1 (Koradi et al. 1996).

Results

Protonation behaviour of side-chain carboxyl groups in RNase T_1

Modified 2D CT-H(CA)CO experiments (Powers et al. 1991; Yamazaki et al. 1994) were performed from pH 9.6

to 2.1 to probe the titration behaviour of the RNase T_1 aspartate and glutamate carboxyl groups. A representative spectrum at pH 5.5 displaying the region of the cross peaks between the side-chain carboxyl and carboxamide carbons and the adjacent protons is shown in Fig. 1. All of the 12 acidic amino acid residues present in RNase T_1 could be unambigously identified in this spectrum by using the resonance assignment of the enzyme at pH 5.5 and 313 K (Pfeiffer et al. 1996). The pH dependence of the chemical shifts of the side chain carboxyl carbon resonances is presented in Fig. 2. The corresponding pK_a values derived from fitting ideal titration curves with up to three pK_a values to the titration data are summarized in Table 1. When more than one pK_a value was required for a reasonable fit, the residue(s) assumed to contribute to this titration behaviour are listed.

Most of the side chain carboxyl carbon resonances in RNase T_1 show a titration behaviour which is well known from model compounds (Keim et al. 1973; Richarz and Wüthrich 1978). As seen in Fig. 2, all of these resonances undergo a downfield shift with increasing pH. However, the $^{13}C^{\delta}$ resonances of E46 and E58 experience a small and the E82 $^{13}C^{\delta}$ resonance a more distinct reverse shift at higher pH values. In general, the chemical shift of the $^{13}C^{\gamma}$ ($^{13}C^{\delta}$) resonance of aspartate (glutamate) residues in RNase T_1 appear between 175 and 177 ppm (179 and 181 ppm) in the protonated state and between 179 and 181 ppm (183 and 185 ppm) in the deprotonated state, with pH titration shifts (δ_b–δ_a) in the range of 3.5–4.5 ppm (3.9–4.7 ppm). It is of interest to note that, in comparison with all the other glutamates, the E58 $^{13}C^{\delta}$ resonance undergoes a substantial smaller pH titration shift (δ_b–δ_a = 3.1 ppm). In addition, both its limiting chemical shifts δ_a and δ_b are shifted upfield by 2 ppm or more. Furthermore, unlike the other resonances illustrated in Fig. 2, the D76 $^{13}C^{\gamma}$ resonance shows very little change in chemical shift in the investigated pH range [δ(pH 9.6)–δ(pH 2.1) = 0.6 ppm]. As a result, the pK_a value of D76 could not be obtained by fitting the experimental data to a modified Henderson-Hasselbalch equation. The question of whether the pK_a value of this buried residue is smaller than 2 or higher than 10 will be discussed below.

In contrast to the side-chain carboxyl carbons, the chemical shifts of the preceding methylene protons could not be utilized for a reliable pK_a determination, owing to the overlap of resonances in corresponding ^{1}H-^{13}C correlated 2D NMR spectra at several pH values and to a more complex titration behaviour. The pH-dependent analysis of the side-chain carboxamide carbon resonances and the backbone carbonyl carbon resonances of observable glycine residues and N81 revealed chemical shift changes smaller than 0.3 ppm and 0.5 ppm, respectively, except for N44. This side-chain carboxamide carbon resonance showed an upfield shift of 1 ppm with

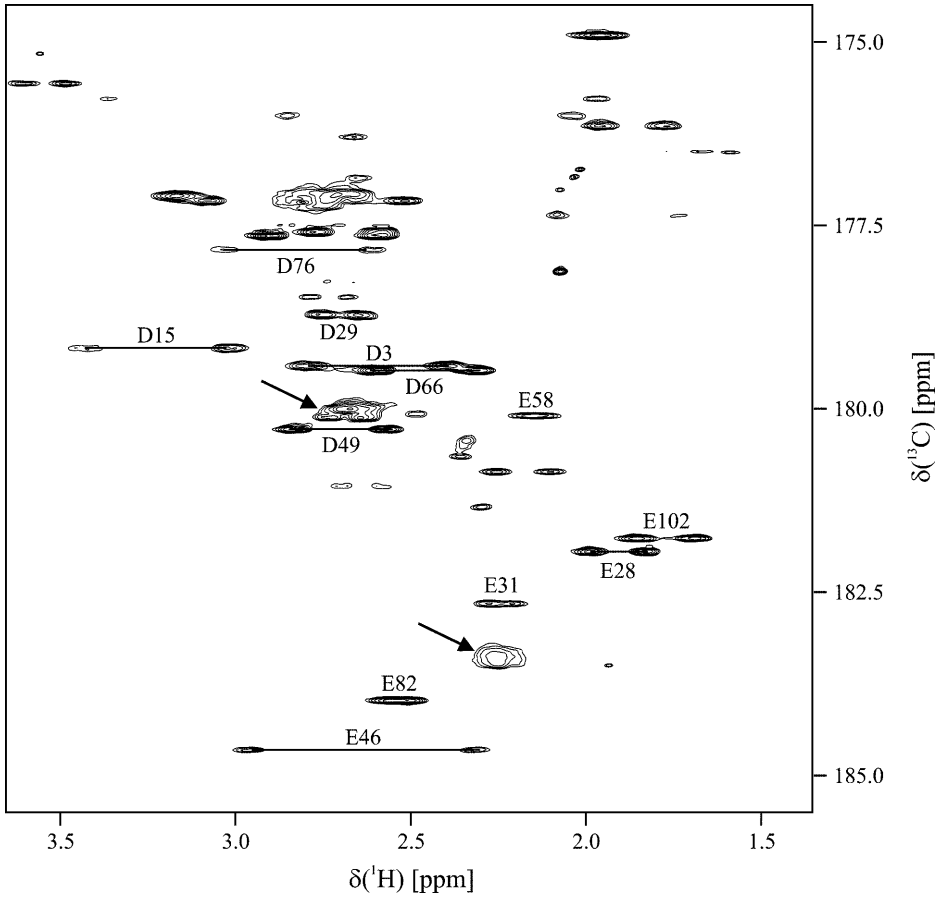

Fig. 1 Portion of a ^{13}CO-^{1}H correlation spectrum of uniformly ^{13}C- and ^{15}N-labelled RNase T_1 at pH 5.5, obtained by using a modified 2D CT-H(CA)CO experiment. The region shown contains the cross peaks for the $^{1}H^{\beta}(^{13}C^{\beta})^{13}C^{\gamma}$ and $^{1}H^{\gamma}(^{13}C^{\gamma})^{13}C^{\delta}$ connectivities of all Asx and Glx residues in the enzyme. Peak assignments for the side-chain carboxyl groups are denoted by one-letter amino acid code and residue number. The broad cross-peaks marked by *arrows* are presumed to correspond to aspartate and glutamate resonances of alkaline denatured RNase T_1

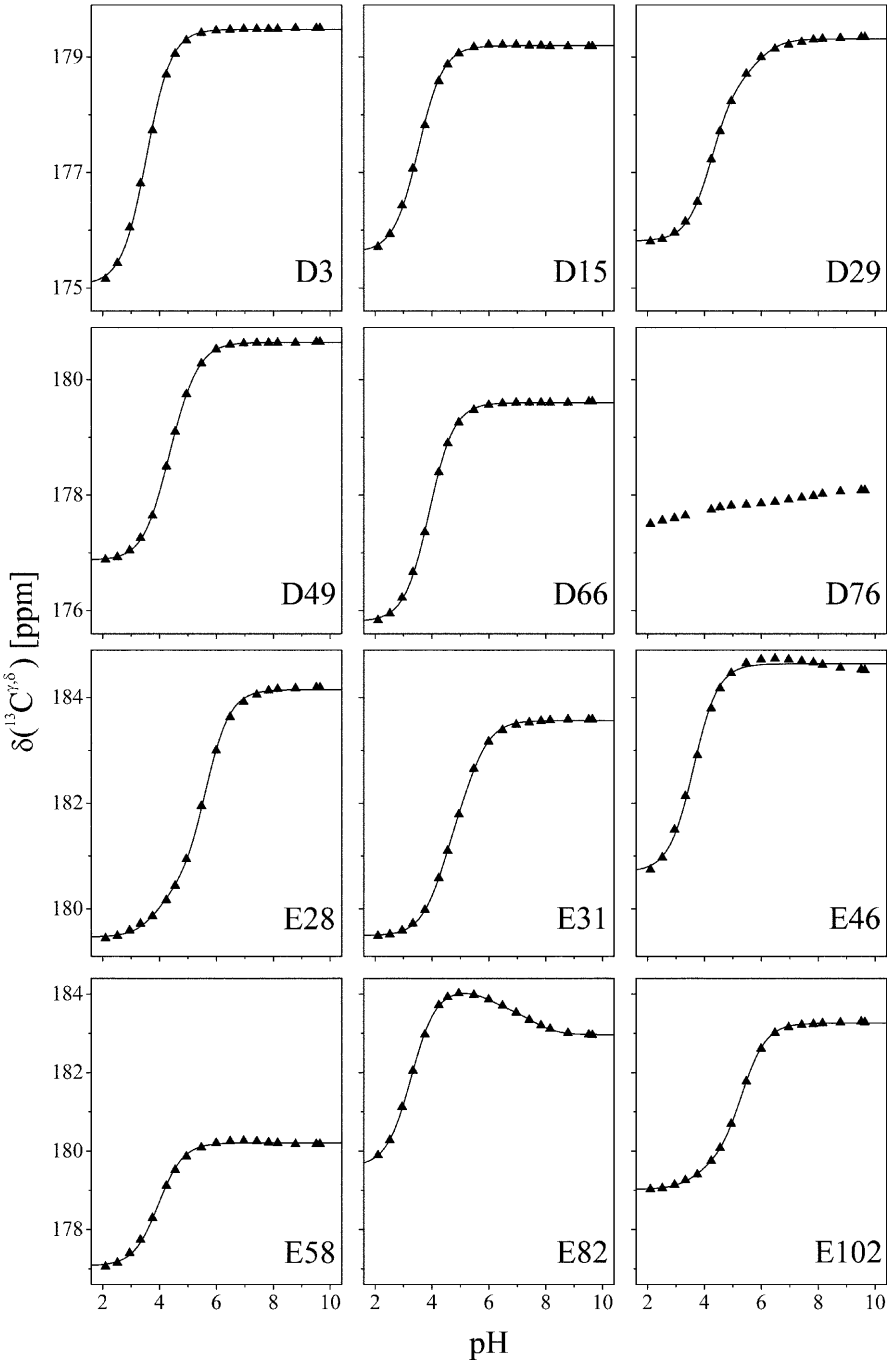

Fig. 2 pH dependence of the chemical shifts of the carboxyl carbon resonances for all side-chain carboxyl groups in native RNase T_1. Experimental data points are indicated by *black triangles*, while *solid lines* represent nonlinear least-squares fits of the data to Eq. (1) with one ($i=1$; D3, D15, D66, E46, E58), two ($i=2$; D29, D49, E28, E31, E102), or three ($i=3$; E82) apparent pK_a values. The obtained pK_a values are listed in Table 1

increasing pH, characterized by a pK_a value of 3.6. Chemical shift data obtained in a test of reversibility by returning the acidified NMR sample to pH 9.6 were superimposable on those measured in the first 2D CT-H(CA)CO experiment of the pH titration at the same pH.

Protonation behaviour and tautomeric states of histidines in RNase T_1

Besides the determination of side-chain carboxylate pK_a values, the identification of the tautomeric states of deprotonated histidine residues was a further main objective of this study. Usually, ^{15}N-labelled protein is utilized in such an investigation by performing a two-dimensional ^{1}H-^{15}N correlation experiment at a pH value above the pK_a values of the individual histidine residues (Pelton et al. 1993). However, as mentioned in the introduction, previous NMR studies have indicated that it is difficult to follow the pH dependence of the imidazole ^{15}N resonances of RNase T_1 owing to extensive line broadening beyond pH 7 (Schmidt 1990). In view of this result, the pH dependence of ^{13}C imidazole resonances was observed to assess the protonation

Table 1 Apparent pK_a values of aspartate and glutamate residues in native RNase T_1 as determined by NMR using the carboxylate carbon resonances

Residue	pK_a	Additional titration events[a]
D3	3.54 ± 0.02	–
D15	3.52 ± 0.02	–
E28	5.61 ± 0.03	D29 (3.90 ± 0.15/0.18 ± 0.02)
D29	4.26 ± 0.03	E28 (5.91 ± 0.12/0.18 ± 0.02)
E31	5.36 ± 0,07	D29 (4.38 ± 0.06/0.57 ± 0.06)
E46	3.62 ± 0.04	–
D49	4.22 ± 0.05	E102 (4.94 ± 0.13/0.24 ± 0.08)
E58	3.96 ± 0.03	–
D66	3.90 ± 0.01	–
D76[b]	–	–
E82	3.27 ± 0.02	H27 (7.57 ± 0.12/–0.19 ± 0.03)
		E28 (6.02 ± 0.16/–0.16 ± 0.03)
E102	5.30 ± 0.02	D49 and/or T104 (3.72 ± 0.13/0.14 ± 0.02)

[a]When two or three pK_a values were required for a reasonable fit, the residue(s) assumed to cause this additional inflections are listed. pK_a and C_i values obtained for this inflection(s) are given in parentheses

[b]The C^{γ} resonance as well as the H^{β} resonances of D76 exhibit no significant titration shift, implying that the pK_a value of this residue is outside the experimental pH range

behaviour and the tautomeric states of the histidine residues.

Among the histidine carbon resonances, the $^{13}C^{\gamma}$ resonance is the most sensitive to the tautomeric state (Reynolds et al. 1973; Walters and Allerhand 1980). Therefore, the CT-H(CD)CG^{His} experiment was developed to observe such resonances in a quick and selective manner. Starting from previously identified $^{1}H^{\delta 2}$, $^{13}C^{\delta 2}$ and $^{15}N^{\varepsilon 2}$ imidazole resonances (Schmidt et al. 1991; Pfeiffer et al. 1996), the assignment of $^{13}C^{\gamma}$ resonances to individual histidine residues was easily achieved at pH 5.5 by careful alignment of the CT-H(CD)CG^{His} spectrum with both the CT-H(C)N and the ^{1}H-^{13}C CT-HSQC spectrum, as demonstrated in Fig. 3. With this aim in view, first of all the $^{1}H^{\delta 2}$-$^{13}C^{\delta 2}$ histidine cross-peaks were identified in the CT-HSQC spectrum. This was easily accomplished because $^{1}H^{\delta 2}$-$^{13}C^{\delta 2}$ histidine and $^{1}H^{\delta 1}$-$^{13}C^{\delta 1}$ tryptophan cross-peaks are of opposite sign relative to the remaining signals in ^{1}H-^{13}C CT-HSQC spectra acquired with a total constant-time delay $T = 1/J_{CC}$ (Vuister and Bax 1992; Plesniak et al. 1996). Afterwards the $^{1}H^{\delta 2}$-$^{13}C^{\delta 2}$ histidine cross-peaks were connected to the $^{1}H^{\delta 2}$-$^{13}C^{\gamma}$ histidine cross-peaks in the CT-H(CD)CG^{His} spectrum, establishing the $^{13}C^{\gamma}$ resonance assignment of all histidine residues in RNase T_1. Finally, the CT-H(C)N spectrum was used to confirm the assignments.

The pH dependence of the imidazole carbon resonances of RNase T_1 is shown in Fig. 4. The pK_a values derived from these data are presented in Table 2. pK_a values determined from the pH dependence of the imidazole proton resonances showed no significant deviations from those of the carbon resonances. From examination of the titration curves it seems evident that the titration behaviour of the three histidines is complex in comparison with that of model compounds (Reynolds et al. 1973; Richarz and Wüthrich 1978). Usually the $^{13}C^{\delta 2}$ and $^{13}C^{\varepsilon 1}$ resonances shift downfield upon deprotonation of the imidazole ring. In fact this is the case for all three histidines of RNase T_1, albeit the $^{13}C^{\delta 2}$ resonance of H92 as well as the $^{13}C^{\gamma}$ resonance could not be followed at pH values above pH 7. Some of the imidazole carbon resonances exhibit additional titration shifts at low pH values, which have been attributed to neighbouring acidic side chains (Table 2).

Inspection of the $^{13}C^{\gamma}$ chemical shift-pH profile yields information about the tautomeric state of the deprotonated histidine ring because, with increasing pH, the $^{13}C^{\gamma}$ resonance shifts upfield or downfield in proportion as the $N^{\delta 1}$-H or the $N^{\varepsilon 2}$-H tautomer is formed (Reynolds et al. 1973). For this, further evidence is provided by the magnitude of the titration shift of the $^{13}C^{\delta 2}$ resonance. While H27 forms predominantly the $N^{\varepsilon 2}$-H tautomer monitored by the downfield shift of the $^{13}C^{\gamma}$ resonance and a small titration shift of the $^{13}C^{\delta 2}$ resonance (~1 ppm), H40 forms mainly the $N^{\delta 1}$-H tautomer according to the observed upfield shift of the $^{13}C^{\gamma}$ resonance and the large titration shift about 6 ppm of the $^{13}C^{\delta 2}$ resonance (Fig. 4).

In the CT-HSQC spectra it was also possible to follow the pH dependence of some other aromatic carbon resonances as those of the histidines. Most of these resonances revealed chemical shift changes less than 0.7 ppm. However, the W59 $^{13}C^{\delta 1}$ resonance showed an upfield shift of about 1.2 ppm, characterized by a pK_a value of 3.9. The largest titration shift with 1.9 ppm was observed for the $^{13}C^{\varepsilon}$ resonance of Y42. A pK_a value of 3.7 could be derived from the downfield shift of this resonance with increasing pH.

Discussion

In Fig. 5 the titratable groups of RNase T_1 for the pH range 2–9 according to their location in the crystal structure are depicted. Half of the titration curves of the aspartate and glutamate residues in Fig. 2 reflect single protonation sites (see also Table 1). However, some of the pK_a values of the carboxylate groups deviate considerably from values expected for solvent-accessible residues which are not significantly influenced by the protein environment. In particular for E28, D29 and E31, a complex titration behaviour and relatively high pK_a values were observed, which is most likely due to their mutual interactions and to the influence of the closely situated C-terminal end of the α-helix. The role of the α-helix termini on the ionization behaviour of titratable groups is well documented (Hol et al. 1978; Karshikoff et al. 1993). Owing to the electrostatic influence of the protein charge multipole, the observed pK_a values of E46 and E102 are shifted to relatively low and higher values, respectively. On the other hand, D3, D15 and D66 exhibit an ideal titration behaviour according to the classical Henderson-Hasselbalch equation. In particular, the pK_a value of the solvent-exposed

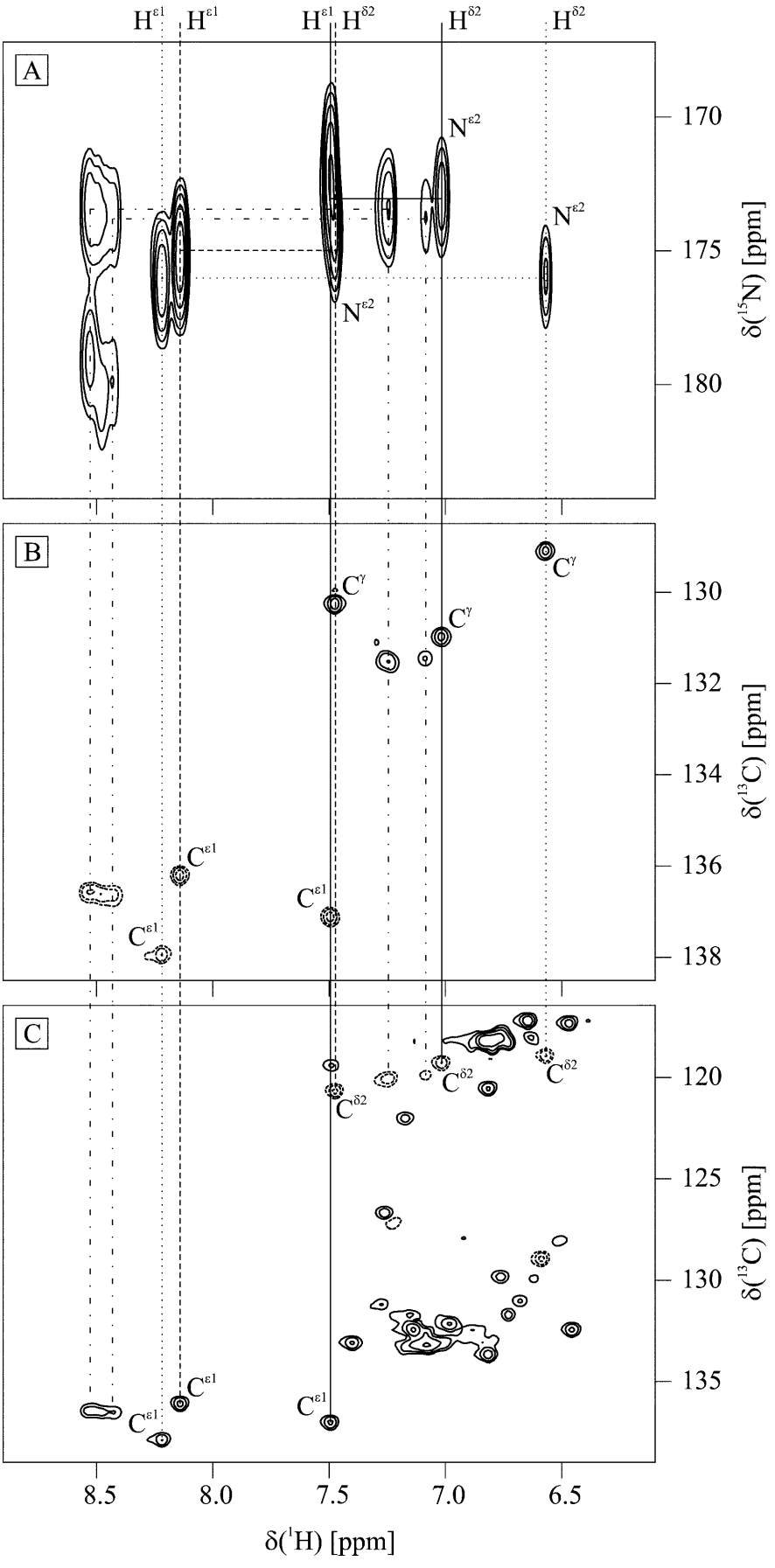

Fig. 3A–C Two-dimensional heteronuclear NMR correlation spectra used to assign the C^{γ} resonances of the three histidine residues in RNase T_1 at pH 5.5 starting from previously identified imidazole ring resonance frequencies (Schmidt et al. 1991; Pfeiffer et al. 1996). Correlations for H27, H40, and H92 are indicated by *dotted*, *dashed*, and *solid lines*, respectively. Peak assignments to ^{1}H, ^{13}C, and ^{15}N resonances are indicated. Cross peaks connected by *dashed-and-dotted lines* are presumed to correspond to histidine resonances of alkaline-denatured RNase T_1. *Broken contours* correspond to negative intensities. **A** Expanded region of the CT-H(C)N spectrum showing ^{1}H-^{15}N correlations in imidazole rings obtained by stepwise coherence transfer through $^{1}J_{CH}$ and $^{1}J_{CN}$ spin couplings. **B** CT-H(CD)CG^{His} spectrum allowing the identification of the histidine C^{γ} resonances and their assignment to individual histidine residues by careful alignment of this spectrum with the CT-H(C)N (**A**) and the CT-HSQC spectrum (**C**). In addition to the histidine $^{1}H^{\delta2}$-$^{13}C^{\gamma}$ cross peaks, only histidine $^{1}H^{\varepsilon1}$-$^{13}C^{\varepsilon1}$ auto peaks with negative intensity appear in the CT-H(CD)CG^{His} spectrum. **C** ^{1}H-$^{13}C^{ar}$ CT-HSQC spectrum, indicating $^{1}H^{\delta1}$-$^{13}C^{\delta2}$ and $^{1}H^{\delta2}$-$^{13}C^{\delta2}$ cross peaks of tryptophan and histidine residues with opposite sign relative to the remaining signals owing to the use of a total constant-time delay $T = 1/J_{CC}$

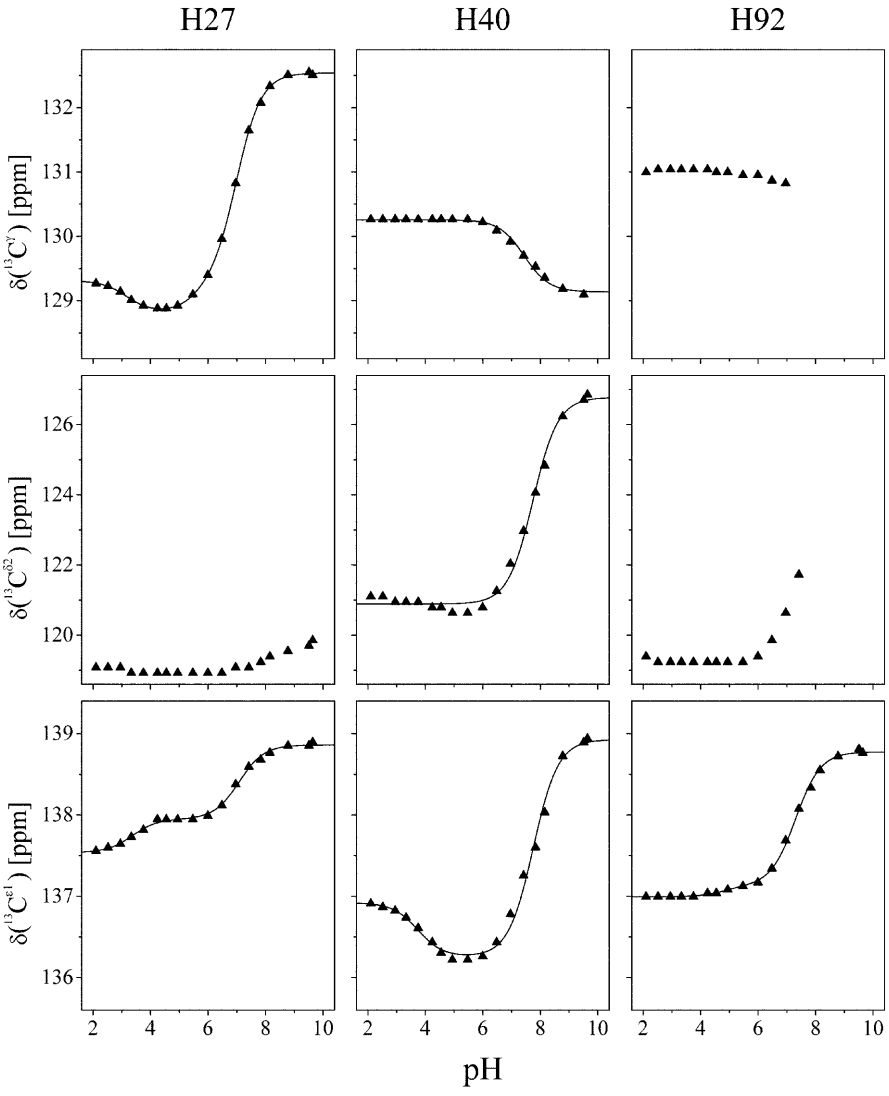

Fig. 4 pH dependence of the chemical shifts of the imidazole carbon resonances in native RNase T_1. Experimental data points are indicated by *black triangles*, while *solid lines* represent nonlinear least-squares fits of the data to Eq. (1) with one ($i = 1$; C^{γ} and $C^{\delta 2}$ of H40), two ($i = 2$; $C^{\varepsilon 1}$ of H27, H40, and H92), or three ($i = 3$; C^{γ} of H27) apparent pK_a values. These values are listed in Table 2. Furthermore, the tautomeric states of the deprotonated histidine residues, obtained by inspection of the ^{13}C chemical shift-pH profiles, are also included in Table 2

Table 2 Apparent pK_a values and tautomeric states of histidine residues in native RNase T_1 as determined by NMR using the imidazole carbon resonances

	Reporter nucleus	pK_a	Additional titration events[a]	Tautomeric state	Reported pK_a values[b]
H27[c]	$^{13}C^{\gamma}$	6.99 ± 0.03	E82 (3.17 ± 0.10/-0.16 ± 0.03) E28 (5.59 ± 0.21/0.13 ± 0.03)	$N^{\varepsilon 2}$-H	7.1[e], 7.26[f]
	$^{13}C^{\varepsilon 1}$	7.08 ± 0.05	E82 (3.36 ± 0.12/0.31 ± 0.02)		
H40	$^{13}C^{\gamma}$	7.44 ± 0.05	–	$N^{\delta 1}$-H	7.7[e], 7.92[f]
	$^{13}C^{\delta 2}$	7.72 ± 0.05	–		
	$^{13}C^{\varepsilon 1}$	7.75 ± 0.05	E58 (3.73 ± 0.22/–0.33 ± 0.05)		
H92[d]	$^{13}C^{\varepsilon 1}$	7.31 ± 0.04	E58 (4.82 ± 0.35/0.07 ± 0.02)	$N^{\delta 1}$-H	7.4[e], 7.80[f]

[a]When two or three pK_a values were required for a reasonable fit, the residue(s) assumed to cause this additional inflections are listed. pK_a and C_i values obtained for this inflection(s) are given in parentheses

[b]Determined from the pH dependence of imidazole proton resonances

[c]Owing to the relative small chemical shift variation with pH, no reliable pK_a value could be derived from the $C^{\delta 2}$ resonance

[d]pK_a values could not be obtained from the pH dependence of the C^{γ} and $C^{\delta 2}$ resonance owing to line broadening beyond detection above pH 7

[e]From Steyaert et al. (1990) (1 mM RNase T_1 in D_2O, 100 mM NaCl, 308 K)

[f]From Inagaki et al. (1981) (2.5 mM RNase T_1 in D_2O, 200 mM NaCl, 296 K)

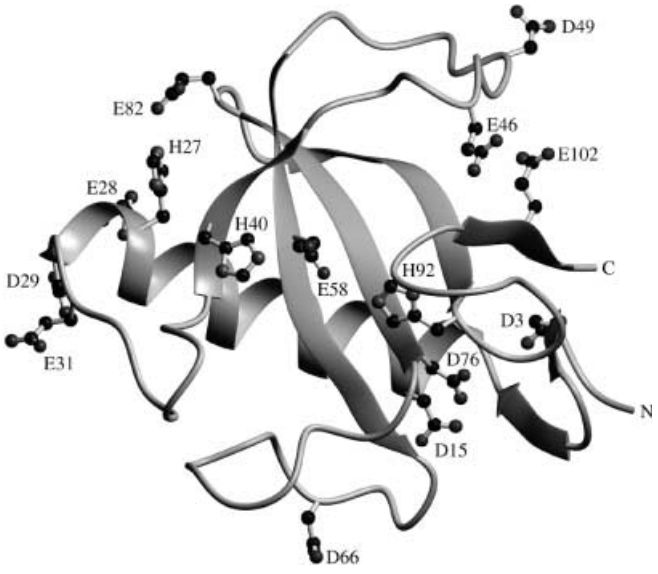

Fig. 5 Ribbon diagram of the crystal structure of RNase T_1 (Martinez-Oyanedel et al. 1991). The protein consists of a central antiparallel five-stranded β-sheet, a short two-stranded β-sheet near the N-terminus, and a peripheral regular α-helix, connected by loop or turn regions. Aspartate, glutamate, and histidine side-chains are illustrated in *ball-and-stick* representation of the heavy atoms. *N* and *C* denote the amino-terminal and carboxy-terminal ends of the peptide chain

carboxylate group of D66, which is distant from all other titratable groups in RNase T_1, corresponds exactly with that found in model compounds (Keim et al. 1973; Richarz and Wüthrich 1978). The low pK_a values of D3 and D15 may be attributed to the location of these residues at the N-terminal end of the α-helix. The titration curve of E82 reflects the ionization of its carboxylate group and the protonation of H27. The pK_a value of the E82 carboxylate group was found to be shifted to lower values and the H27 pK_a shifted to higher values owing to the direct interaction of the two groups. The unusual values of the chemical shift of the E58 carboxyl $^{13}C^{\delta}$ resonance, as well as the smaller difference between the protonated and deprotonated state, indicates an unusual environment of this residue. Its pK_a value was found to be relatively low. Although some of the titration curves of H40 reflect the ionization of E58, the $^{13}C^{\delta}$ resonance of the E58 carboxylate shifts only slightly in the pH range of the H40 ionization.

As described in the Materials and methods section, mainly F-test statistics were used to assess the number *i* of deprotonation/protonation processes contributing to the chemical shift-pH profile of a reporter nucleus. Furthermore, owing to the uncertainty in the chemical shift determination of ^{13}C resonances, only those curve fittings were taken into account for which each titration step $C_i(\delta_a–\delta_b)$ exceeded approximately 0.2 ppm. Usually the pK_a value belonging to the largest titration step of the selected fit was assigned to the titratable group being part of the amino acid residue of the reporter nucleus itself, while the minor steps were attributed to neighbouring titratable groups with appropriate pK_a values as judged by inspection of both the crystal structure (PDB code 9RNT) and the NMR structure ensemble (PDB code 1YGW). For example, this procedure resulted in the selection of the fit with two pK_a values for the E28 C^{δ} resonance, and the pK_a value of the minor titration step was attributed to the nearby carboxylate group of D29 (Table 1). The carboxylate oxygen atoms of this residue are 5.9 and 7.2 Å distant from the E28 carboxylate carbon atom in the crystal structure. In the case of the E31 C^{δ} resonance, the above-mentioned criteria would result in a pK_a value of 4.4 for the carboxylate group of E31 and a pK_a of 5.4 for the relatively large minor titration step ($C_2 = 0.43 \pm 0.06$). Starting from this, the carboxylate group of E28 is the only possible candidate to cause the minor inflection. However, the large distance between these two carboxylate groups (about 13 Å) makes it unlikely that the carboxylate group of E28 causes such a large shift in the titration curve of the E31 C^{δ} resonance. On the other hand, there is a possibility that the pK_a value of the minor step has to be assigned to the carboxylate group of E31. Assuming this, it is reasonable to attribute the major titration step to the titratable group of D29, which is only about 7 Å apart from the carboxylate group of E31. The large shift of this step is presumably the result of conformational changes caused by the titration of the carboxylate group of D29. This assumption is supported by the findings of Walter et al. (1995) and Myers et al. (1996). Walter et al. (1995) investigated the pH dependence of the stability of wild-type RNase T_1 and the D29N mutant by thermal unfolding experiments. However, the difference in unfolding free energy between the mutant and the wild-type protein revealed a complex behaviour in dependence on pH, indicating that pH-dependent events additional to the change in the charge state of D29 were lost in the mutant enzyme. A clue about residues responsible for the additional interactions in the wild-type enzyme was obtained by the investigation of changes in the helix content with pH for peptides based on the sequence of the α-helix of RNase T_1 (residues 13 to 29 in the protein) (Myers et al. 1996). By comparison of their results with those of Walter et al. (1995), Myers et al. concluded that part of the additional (destabilizing) effect of D29 in wild-type RNase T_1 is caused by residues outside of the helix and that E31 is a likely candidate for such an interaction. These findings corroborate the assumption that in the case of the E31 C^{δ} resonance the minor titration step is caused by its own carboxylate group.

From the pH dependence of the D76 carboxylate carbon resonances there is no indication that this carboxylate group is deprotonated or protonated in the investigated pH range. The value of the $^{13}C^{\gamma}$ chemical shift resembles that of a protonated carboxylate group (Yamazaki et al. 1994; Qin et al. 1996; Pfeiffer et al. 1998). A transfer of the protein to D_2O solution should be connected with a small upfield shift ($\sim$0.2 ppm) in resonance position of the carboxyl ^{13}C resonance in the

case when the carboxylate is deuterated to a neutral species (Hansen 1983). Within the margin of error, only a small shift of the D76 $^{13}C^{\gamma}$ resonance has been observed. Either the D76 protonated carboxylate group is not accessible in D_2O or other effects may prevent a larger shift of the carboxylate ^{13}C resonance. In an earlier investigation a charged form of D76 has been suggested from a comparison of the pH dependence of the stability of wild-type RNase T_1 and the D76N mutant (Giletto and Pace 1999). However, in the following paper it will be demonstrated that the D76 carboxylate group should have an extremely high pK_a value (about 6.5), which results from its low solvent accessibility and the strong electrostatic interactions with neighbouring groups.

The pK_a values of the three histidine residues determined in this study agree well with those from former investigations (Table 2). The higher pK_a values of Inagaki et al. (1981) may be mainly a result of the lower temperature, because histidines are titrated with high ionization enthalpies. The $^{13}C^{\gamma}$ and $^{13}C^{\delta 2}$ chemical shift-pH profiles of the histidines (Fig. 4) suggest that the deprotonated H27 exists predominantly as the $N^{\varepsilon 2}$-H tautomer, while H40 predominantly exists in the rare $N^{\delta 1}$-H form. In the active site near H40, different hydrogen bond patterns were observed by NMR and X-ray analysis. The result of the tautomer formation found here is in good agreement with the structural data derived by means of NMR spectroscopy, and rules out a strong hydrogen bond between H40 $H^{\varepsilon 2}$ and the carboxylate oxygens of E58. Further evidence for this comes from the pH dependence of the $^{13}C^{\delta}$ resonance of E58, which does not show a strong reflection of the H40 pK_a as in the case of the titration curves of H27 and E82. The dramatic line broadening of the $^{13}C^{\gamma}$ and $^{13}C^{\delta 2}$ resonances of H92 at higher pH values indicates a chemical exchange which is relatively slow on the NMR time scale. It may be possible that the line broadening indicates a slow exchange between the $N^{\delta 1}$-H and the $N^{\varepsilon 2}$-H tautomer. However, by comparing all histidine C^{γ} and $C^{\delta 2}$ chemical shift-pH profiles it seems to be evident that H92 forms predominantly the rare $N^{\delta 1}$ tautomer. Like for H40, the C^{γ} resonance of H92 shows only a small upfield shift and the $C^{\delta 2}$ resonance a large downfield shift with increasing pH. This finding is in good agreement with the X-ray structure (Martinez-Oyanedel et al. 1991), for which a hydrogen bond between H92 $H^{\delta 1}$ and the N99 O has been reported.

As mentioned in the Results section, the C^{ε} resonance of Y42, the C^{γ} resonance of N44, and the $C^{\delta 1}$ resonance of W59 showed relatively large titration shifts. It is evident that the pK_a values derived from these titration shifts cannot be attributed to a protonation/deprotonation process of these residues. Rather, such a shift is the result of the change in the protonation state of a nearby titratable group and/or pH-dependent conformational changes such as the reorganization of a hydrogen bond network or the shifting of a conformational equilibrium. Unfortunately, there are no structural data at acidic pH (about pH 3) available for RNase T_1. Therefore, an interpretation of the above-mentioned titration shifts of Y42, N44, and W59 should be speculative. However, it is worth stating at this point that Y42 and N44 are part of the guanine recognition site (residues 42 to 46 and 98). Moreover, it is striking that the pK_a value of E46 (3.62 ± 0.04) practically coincides with the values obtained for the Y42 C^{ε} resonance (3.69 ± 0.07) and the N44 C^{γ} resonance (3.61 ± 0.05). In view of the distance between these two residues and E46 (about 9 Å each, measured from the reporter nuclei to the E46 carboxylate oxygen atoms), it is unlikely that the large titration shifts of these resonances reflect only direct through-space electrostatic effects. It seems to be more reasonable to assume that these shifts are the result of (local) conformational changes, due to the change in the state of ionization of E46. From a comparison of crystal stuctures of nucleotide-free RNase T_1 (Kostrewa et al. 1989; Martinez-Oyanedel et al. 1991) and its complex with 2′-GMP (Arni et al. 1988) it was concluded that the binding of guanine is accompanied by several induced-fit-type conformational changes. The most striking features of the induced fit are a 140° flip of the N43-N44 peptide group and a rotation about the C^{α}-C^{β} bond of E46 to bring its carboxylate group closer to the recognition pocket. In addition, these changes break down the hydrogen bond between Y42 O^{η}-H and N44 O^{δ}. However, NMR studies revealed that the different conformations found in crystal structures of complexed and nucleotide-free RNase T_1 are already present in solution in the absence of a substrate (Fushman et al. 1994; Pfeiffer et al. 1997). These considerations imply that the equilibrium of the conformations in the recognition loop is, to some extent, pH modulated. On the other hand, X-ray studies of E46Q RNase T_1 (which may be a suitable model of a protonated glutamate) in complex with 2′-GMP or 2′-AMP showed that the recognition site adopts essentially the same geometry as in the crystal structure of nucleotide-free RNase T_1 (Granzin et al. 1992). This surprising result is caused by the formation of a hydrogen bond between a side-chain amide proton of Q46 and the backbone carbonyl oxygen of F100, permitting the induced-fit-type conformational changes. Owing to these conformational changes, the recognition loop is locked and the guanine base binds at the 3′ subsite. Interestingly, there is no hydrogen bond between Y42 O^{η}-H and N44 O^{δ} in the E46Q mutant/2′-GMP complex. These findings allow an alternative interpretation of the titration shifts observed for the Y42 C^{ε} resonance and the N44 C^{γ} resonance. Accordingly, the protonation of E46 induces the formation of a hydrogen bond between this protonated carboxylate group and the backbone carbonyl oxygen of F100, resulting in the loss of the hydrogen bond between Y42 O^{η}-H and N44 O^{δ}.

The individual pK_a values determined in this work represent a basis for understanding the pH dependence of stability and activity of RNase T_1. The analysis of the activity/pH plot revealed that two groups in its

deprotonated form and two groups in its protonated state are required for full enzymatic activity (Osterman and Walz 1978; Steyaert et al. 1990). It was concluded that H40 and H92 represent the protonated groups, while E58 and an unidentified carboxylate group correspond to the deprotonated groups. These findings and the pK_a values derived from the analysis of the activity/pH plot are in good agreement with the results presented here. In view of the above discussion concerning the recognition site, E46 is an attractive candidate for the unknown deprotonated group. In the following paper the structural features of all investigated side chains will be discussed in detail.

Acknowledgements The investigation was financially supported by a specific RTD project in the biotechnology research and technological development program of the European Community (BIO4CT970129). We would like to thank Dr. David Fushman, Department of Chemistry and Biochemistry, University of Maryland, for making available to us the F-test MATLAB routine.

References

Arni R, Heinemann U, Tokuoka R, Saenger W (1988) Three-dimensional structure of the ribonuclease T_1*2′-GMP complex at 1.9-Å resolution. J Biol Chem 263:15358–15368

Bax A, Pochapsky SS (1992) Optimized recording of heteronuclear multidimensional NMR spectra using pulsed field gradients. J Magn Reson 99:638–643

Blomberg F, Maurer W, Rüterjans H (1977) Nuclear magnetic resonance investigation of ^{15}N-labeled histidine in aqueous solution. J Am Chem Soc 39:8149–8159

Bradbury JH, Scheraga HA (1966) Structural studies of ribonuclease. XXIV. The application of nuclear magnetic resonance spectroscopy to distinguish between the histidine residues of ribonuclease. J Am Chem Soc 88:4240–4246

Edsall JT, Martin RB, Hollingworth BR (1958) Ionization of individual groups in dibasic acids, with application to the amino and hydroxyl groups of tyrosine. Proc Natl Acad Sci USA 44:505–519

Fülling R, Rüterjans H (1978) Proton magnetic resonance studies of ribonuclease T_1. Assignment of histidine-27 C2-H and C5-H proton resonances by a photooxidation reaction. FEBS Lett 88:279–282

Fushman D, Ohlenschläger O, Rüterjans H (1994) Determination of the backbone mobility of ribonuclease T1 and its 2′-GMP complex using molecular dynamics simulations and NMR relaxation data. J Biol Struct Dyn 11:1377–1402

Giletto A, Pace CN (1999) Buried, charged, non-ion-paired aspartic acid 76 contributes favorably to the conformational stability of ribonuclease T_1. Biochemistry 38:13379–13384

Gilson MK (1995) Theory of electrostatic interactions in macromolecules. Curr Opin Struct Biol 5:216–223

Granzin J, Puras-Lutzke R, Landt O, Grunert H-P, Heinemann U, Saenger W, Hahn U (1992) RNase T_1 mutant Glu46Gln binds the inhibitors 2′-GMP and 2′-AMP at the 3′ subsite. J Mol Biol 225:533–542

Grzesik S, Bax A (1993) The origin and removal of artifacts in 3D HCACO spectra of proteins uniformly enriched with ^{13}C. J Magn Reson B 102:103–106

Hansen PE (1983) Isotope effects on nuclear shielding. In: Webb GA (ed) Annual reports on NMR spectroscopy, vol 15. Academic Press, London, pp 105–234

Hol WGJ, van Duijnen PT, Berendsen HJC (1978) The α-helix dipole and the properties of proteins. Nature 273:443–446

Inagaki F, Kawano Y, Shimada I, Takahashi K, Miyazama T (1981) Nuclear magnetic resonance study on the microenvironments of histidine residues of ribonuclease T_1 and carboxymethylated ribonuclease T_1. J Biochem (Tokyo) 89:1185–1195

Karshikoff A, Reinemer P, Huber R, Ladenstein R (1993) Electrostatic evidence for the activation of the glutathione thiol by tyrosine 7 p class GSH transferases. Eur J Biochem 215:663–670

Kay LE, Keifer P, Saarinen T (1992) Pure absorption gradient enhanced heteronuclear single quantum correlation spectroscopy with improved sensitivity. J Am Chem Soc 114:10663–10665

Keim P, Vigna RA, Morrow JS, Marshall RC, Gurd FRN (1973) Carbon 13 nuclear magnetic resonance of pentapeptides of glycine containing central residues of serine, threonine, aspartic, and glutamic acids, asparagine, and glutamine. J Biol Chem 248:7811–7818

Koradi R, Billeter M, Wüthrich K (1996) MOLMOL: a program for display and analysis of macromolecular structures. J Mol Graphics 14:51–55

Kostrewa D, Choe H-W, Heinemann U, Saenger W (1989) Crystal structure of guanosine-free ribonuclease T_1, complexed with vanadate(V), suggests conformational change upon substrate binding. Biochemistry 28:7592–7600

Laskowski JR M, Scheraga HA (1954) Thermodynamic considerations of protein reactions. I. Modified reactivity of polar groups. J Am Chem Soc 76:6305–6319

Linderstrøm-Lang K (1924) On the ionisation of proteins. C R Trav Lab Carlsberg 15:1–29

Marion D, Ikura M, Tschudin R, Bax A (1989) Rapid recording of 2D NMR spectra without phase cycling. Application to the study of hydrogen exchange in proteins. J Magn Reson 85:393–399

Markley JL (1975) Observation of histidine residues in proteins by means of nuclear magnetic resonance spectroscopy. Acc Chem Res 8:70–80

Martinez-Oyanedel J, Choe H-W, Heinemann U, Saenger W (1991) Ribonuclease T1 with free recognition and catalytic site: crystal structure analysis at 1.5 Å resolution. J Mol Biol 222:335–352

Meadows DH, Jardetzky O, Epand RM, Rüterjans HH, Scheraga HA (1968) Assignment of the histidine peaks in the nuclear magnetic resonance spectrum of ribonuclease. Proc Natl Acad Sci USA 60:766–772

Motulsky HJ, Ransnas LA (1987) Fitting curves to data using nonlinear regression: a practical and nonmathematical review. FASEB J 1:365–374

Myers JK, Smith JS, Pace CN, Scholtz JM (1996) The α-helix of ribonuclease T_1 as an independent stability unit: direct comparison of peptide and protein stability. J Mol Biol 263:390–395

Nakamura H (1996) Roles of electrostatic interactions in proteins. Q Rev Biophys 29:1–90

Oda Y, Yamazaki T, Nagayama K, Kanaya S, Kuroda H, Nakamura H (1994) Individual ionization constants of all the carboxyl groups in ribonuclease HI from *Escherichia coli* determined by NMR. Biochemistry 33:5275–5284

Osterman HL, Walz Jr FG (1978) Subsites and catalytic mechanism of ribonuclease T_1: kinetic studies using GpA, GpC, GpG, and GpU as substrates Biochemistry 17:4124–4130

Pace CN, Heinemann U, Hahn U, Saenger W (1991) Ribonuclease T_1: structure, function and stability. Angew Chem Int Ed Engl 30:343–360

Palmer AG III, Cavanagh J, Wright PE, Rance M (1991) Sensitivity improvement in proton-detected two-dimensional correlation NMR spectroscopy. J Magn Reson 93:151–170

Pelton JG, Torchia DA, Meadow ND, Roseman S (1993) Tautomeric states of the active-site histidines of phosphorylated and unphosphorylated III^{Glc}, a signal-transducing protein from *Escherichia coli*, using two-dimensional heteronuclear NMR techniques. Protein Sci 2:543–558

Pfeiffer S, Engelke J, Rüterjans H (1996) Complete ^{1}H, ^{15}N and ^{13}C resonance assignment of ribonuclease T_1: secondary structure and backbone dynamics as derived from the chemical shifts. Q Magn Reson Biol Med 3:67–87

Pfeiffer S, Karimi-Nejad Y, Rüterjans H (1997) Limits of NMR structure determination using variable target function calculations: ribonuclease T_1, a case study. J Mol Biol 266:400–423

Pfeiffer S, Spitzner N, Löhr F, Rüterjans H (1998) Hydration water molecules of nucleotide-free RNase T_1 studied by NMR spectroscopy in solution. J Biomol NMR 11:1–11

Piotto M, Saudek V, Sklenár V (1992) Gradient-tailored excitation for single-quantum NMR spectroscopy of aqueous solutions. J Biomol NMR 2:661–665

Plesniak LA, Connelly GP, Wakarchuk WW, McIntosh LP (1996) Characterization of a buried neutral histidine residue in *Bacillus circulans* xylanase: NMR assignments, pH titration, and hydrogen exchange. Protein Sci 5:2319–2328

Powers R, Gronenborn AM, Clore GM, Bax A (1991) Three-dimensional triple resonance NMR of $^{13}C/^{15}N$-enriched proteins using constant-time evolution. J Magn Reson 94:209–213

Qin J, Clore M, Gronenborn AM (1996) Ionization equilibria for side-chain carboxyl groups in oxidized and reduced human thioredoxin and in the complex with its target peptide from the transcription factor NFκB. Biochemistry 35:7–13

Quaas R, McKeown Y, Stanssens P, Frank R, Blöcker H, Hahn U (1988a) Expression of the chemically synthesized gene for ribonuclease T1 in *Escherichia coli* using a secretion cloning vector. Eur J Biochem 173:617–622

Quaas R, Grunert H-P, Kimura M, Hahn U (1988b) Expression of ribonuclease T1 in *Escherichia coli* and rapid purification of the enzyme. Nucleosides Nucleotides 7:619–623

Reynolds WF, Peat IR, Freedman MH, Lyerla JR Jr (1973) Determination of the tautomeric form of the imidazole ring of L-histidine in basic solution by carbon-13 magnetic resonance spectroscopy. J Am Chem Soc 95:328–331

Richarz R, Wüthrich K (1978) Carbon-13 NMR chemical shifts of the common amino acid residues measured in aqueous solutions of the linear tetrapeptides H-Gly-Gly-X-L-Ala-OH. Biopolymers 17:2133–2141

Rüterjans H, Pongs O (1971) On the mechanism of action of ribonuclease T_1. Nuclear magnetic resonance study on the active site. Eur J Biochem 18:313–318

Rüterjans H, Witzel H (1969) NMR studies on the structure of the active site of pancreatic ribonuclease A. Eur J Biochem 9:118–127

Rüterjans H, Witzel H, Pongs O (1969) Proton magnetic resonance studies on ribonuclease T_1. Biochem Biophys Res Commun 37:247–253

Schmidt JM (1990) PhD thesis. University of Frankfurt, Germany

Schmidt JM, Thüring H, Werner A, Rüterjans H, Quaas R, Hahn U (1991) Two-dimensional ^{1}H, ^{15}N-NMR investigation of uniformly ^{15}N-labeled ribonuclease T1. Eur J Biochem 197:643–653

Shaka AJ, Barker PB, Freeman R (1985) Computer-optimized decoupling scheme for wideband applications and low-level operation. J Magn Reson 64:547–552

Shrager RI, Cohen JS, Heller SR, Sachs DH, Schechter AN (1972) Mathematical models for interacting groups in nuclear magnetic resonance titration curves. Biochemistry 11:541–547

Steyaert J (1997) A decade of protein engineering on ribonuclease T_1. Atomic dissection of the enzyme-substrate interactions. Eur J Biochem 247:1–11

Steyaert J, Hallenga K, Wyns L, Stanssens P (1990) Histidine-40 of ribonuclease T_1 acts as a base catalyst when the true catalytic base, glutamic Acid-58, is replaced by alanine. Biochemistry 29:9064–9072

Sudmeier JL, Ash EL, Günther UL, Luo X, Bullock PA, Bachovchin WW (1996) HCN, a triple-resonance NMR technique for selective observation of histidine and tryptophan side chains in $^{13}C/^{15}N$-labeled proteins. J Magn Reson B 113:236–247

Tran-Dinh S, Fermandhan S, Sala E, Mermet-Bouvier R, Cohen M, Fromageot P (1975) Geminal and vicinal ^{13}C-^{13}C coupling constants of 85% ^{13}C-enriched amino-acids. J Am Chem Soc 97:1267–1268

Ullmann GM, Knapp EW (1999) Electrostatic models for computing protonation and redox equilibria in proteins. Eur Biophys J 28:533–551

Vuister GW, Bax A (1992) Resolution enhancement and spectral editing of uniformly ^{13}C-enriched proteins by homonuclear broadband ^{13}C decoupling. J Magn Reson 98:428–435

Walter S, Hubner B, Hahn U, Schmid FX (1995) Destabilization of a protein helix by electrostatic interactions. J Mol Biol 252:133–143

Walters DE, Allerhand A (1980) Tautomeric states of the histidine residues of bovine pancreatic ribonuclease A. J Biol Chem 255:6200–6204

Warshel A, Papazyan A (1998) Electrostatic effects in macromolecules: fundamental concepts and practical modeling. Curr Opin Struct Biol 8:211–217

Wishart DS, Bigam CG, Yao J, Abildgaard F, Dyson HJ, Oldfield E, Markley JL, Sykes BD (1995) ^{1}H, ^{13}C and ^{15}N chemical shift referencing in biomolecular NMR. J Biomol NMR 6:135–140

Yamazaki T, Yoshida M, Nagayama K (1993) Complete assignments of magnetic resonances of ribonuclease H from *Escherichia coli* by double- and triple-resonance 2D and 3D NMR spectroscopies. Biochemistry 32:5656–5669

Yamazaki T, Nicholson LK, Torchia DA, Wingfield P, Stahl SJ, Kaufman JD, Eyermann CJ, Hodge CN, Lam PYS, Ru Y, Jadhav PK, Chang CH, Weber PC (1994) NMR and X-ray evidence that the HIV protease catalytic aspartyl groups are protonated in the complex formed by the protease and a non-peptide cyclic urea-based inhibitor. J Am Chem Soc 116:10791–10792